Int J Clin Exp Pathol 2016;9(7):6846-6856
www.ijcep.com /ISSN:1936-2625/IJCEP0027945

Original Article

Conditioned medium from hypoxia-stimulated placenta-derived mesenchymal stem cells alters the biological properties of fibroblasts in scar formation via IL-10 and STAT3/ERK signaling pathways

Lili Du[1], Runxiao Lv[2,3], Xiaoyi Yang[4], Shaohang Cheng[5], Jing Xu[5], Yanqiu Yu[1]

[1]Department of Pathophysiology, College of Basic Medical Science, China Medical University, Shenyang, People's Republic of China; [2]Graduate Management Unit, The Second Military Medical University, Shanghai, People's Republic of China; [3]Department of Orthopedics, Changhai Hospital of The Second Military Medical University, Shanghai, People's Republic of China; [4]Seven-Year System, Clinical Medicine, China Medical University, Shenyang, People's Republic of China; [5]Department of Dermatology, Shengjing Hospital of China Medical University, Shenyang, People's Republic of China

Received March 11, 2016; Accepted May 25, 2016; Epub July 1, 2016; Published July 15, 2016

Abstract: It is well known that hypertrophic scar formation is correlated with the hyperproliferation of fibroblasts. Mesenchymal stem cells (MSCs) have been demonstrated to be effective in inhibiting scar formation. Here, we investigated the effect of hypoxic conditioned medium from placenta-derived MSCs (PDMSC-hypoCM) on the biological properties of fibroblasts and the possible mechanisms involved. The isolated PDMSCs were identified by flow cytometry. IL-10 expression was measured by Real-time PCR and ELISA after hypoxic treatment. Cell survival and apoptosis of mouse fibroblasts NIH-3T3 was examined by crystal violet staining and Annexin V-FITC/PI staining, respectively. Cell invasion was measured by Transwell assay. MMP-2 and MMP-9 levels were evaluated by Western blot. Then, a mouse model of thermal injury was generated. On day 15, the levels of α-SMA, Ki67 and F4/80 in scar tissues were measured by Immunohistochemical staining. The activation of STAT3 and ERK pathways were investigated. The results showed that the isolated PDMSCs were positive for CD29 and CD44, while negative for CD31, CD34, CD45 and HLA-DR. Hypoxia significantly induced IL-10 expression in PDMSCs. PDMSC-hypoCM and IL-10 decreased the living cell number, promoted NIH-3T3 cell apoptosis, impaired invasion capability, lowered MMP-2 and MMP-9 levels in NIH-3T3 and reduced α-SMA, Ki67, F4/80, p-STAT3 and p-ERK levels in scar tissues in a mouse model. We also observed that the effect of PDMSC-hypoCM *in vitro* and *in vivo* was reversed by neutralizing antibody against IL-10. In conclusion, PDMSC-hypoCM may suppress scar formation via IL-10, STAT3 and ERK pathways.

Keywords: Hypertrophic scar, PDMSC, hypoxia, IL-10, STAT3, ERK

Introduction

Thermal injury is one of the most severe forms of trauma. Thermal injury can induce remarkably physiological changes, including immunosuppression, inflammation and organ dysfunction [1, 2]. Despite a remarkably decrease in mortality, large burns also contribute to prolonged hospital stay and high morbidity [3]. Thermal injury to the deep dermis may cause prolonged inflammation and eventually lead to hypertrophic scar formation [4]. Hypertrophic scar, a common fibroproliferative disorder, is characterized by hypercellularity, collagen production and the deposition of excessive extracellular matrix (ECM) [5, 6]. Fibroblasts are the key "effector cells" in hypertrophic scar [7].

Previous studies reported that mesenchymal stem cells (MSCs) migrated to the wound sites to form the microenvironment, and then promoted wound healing and attenuated scar formation [8, 9]. MSCs are multipotent nonhematopoietic cells with self-renewing properties. They differentiate into mesenchymal and non-mesenchymal lineages [10-12]. Placenta-derived MSCs (PDMSCs) possess similar biological properties with BMMSCs [13]. Moreover, PDMSCs can be easily obtained from placental tissues and have higher proliferation ability

than BMMSCs [14]. Chamber DC et al. found that administration of PDMSCs significantly attenuated idiopathic pulmonary fibrosis in humans [15]. Kong P et al. pointed that human PDMSCs accelerated wound healing rate in diabetic rats through enhancing angiogenesis [16].

Interleukin-10 (IL-10) is a cytokine that has anti-inflammatory, anti-fibrotic and immunosuppressive effects [17, 18]. IL-10 can be produced by various cell types, including eosinophils, mast cells, macrophages, dendritic cells and B cells [19]. IL-10 plays an important role in wound healing and the suppression of scar formation [18, 20]. In the process of scar formation, decreased levels of inflammatory-related genes (IL-1α, TNF-α, IL-10, CCL-2, CCL-3 and CXCR2) were observed in human wounds [21]. Kieran et al. found that IL-10 administration suppressed scar formation in rats and humans [20]. Nowadays, IL-10 has been used as an effective therapeutic agent in the prevention of scarring. Xu L et al. observed that hypoxia significantly increased the expression of IL-10 in adipose-derived mesenchymal stem cells (ADMSCs) compared with the normoxic environment [22]. Chen et al. demonstrated that hypoxia-preconditioned MSCs inhibited the activation of cardiac fibroblasts [23]. Additionally, Lan et al. reported that hypoxia-preconditioned MSC transplantation exerted an effective therapeutic effect on pulmonary fibrosis in mice [24].

STAT3, a multifunctional signaling pathway, functions in cell proliferation, apoptosis, differentiation and inflammation [25]. Additionally, ERK pathway is also associated with cell proliferation, migration and differentiation. Evidences showed that STAT3 and ERK signaling pathways played vital roles in fibrosis [26, 27]. Moreover, hypertrophic scar is characterized by excessive ECM deposition and fibrosis [28]. However, the roles of STAT3 and ERK signaling pathways in scar formation remain unknown.

In our study, we obtained mouse PDMSCs and expanded them *in vitro*. We further investigated the effect of hypoxic conditioned medium from PDMSCs (PDMSC-hypoCM) on the proliferation, apoptosis and invasion of mouse fibroblasts NIH-3T3 *in vitro*. Moreover, we explored the underlying mechanism *in vivo*.

Materials and methods

Isolation of PDMSCs

Placental tissues were obtained from mice under sterile conditions and washed twice with phosphate-buffered saline (PBS). The outer membrane was stripped using ophthalmic scissors and pincette. After washed with PBS, the tissues were minced into 1-3 mm^3 pieces and cultured in the culture flask coated with a thin layer of FBS at 37°C in a 5% CO_2 humanized atmosphere. Then, DMEM (Gibco, Grand Island, NY, USA) containing 10% FBS (GE Healthcare HyClone, Logan, UT, USA) was added after 12 h of culture. The cell number was counted and subcultured when PDMSCs grown out from the placental tissues.

Characterization of PDMSCs

After grown to 80% confluence, the cells were washed and trypsinized. The cell suspension was centrifuged at 1000 rpm for 3 min and resuspended in PBS. The cell density was 1×10^6 cells/ml. The cells (1×10^6 cells) were washed, resuspended in 100 μl PBS, incubated with 5 μl FITC labeled antibodies against CD29, CD31, CD34, CD44, CD45 and HLA-DR (all purchased from eBioscience, San Diego, CA, USA) at room temperature for 30 min in the dark and analyzed by flow cytometer C6 (BD, Franklin Lakes, NJ, USA).

Collection of conditioned medium

PDMSCs were cultured for 3 days under normoxic (20% O_2) and hypoxic (5% and 1% O_2) conditions. The conditioned medium from normoxia- and hypoxia-stimulated PDMSCs were named PDMSC-norCM and PDMSC-hypoCM, respectively.

Enzyme-linked immunosorbant assay (ELISA)

The cell culture supernatant was collected after hypoxic treatment and the expression of interleukin (IL)-10 in the supernatant was measured by ELISA according to the manufacturer's protocol (WHB-Bio, Shanghai, China).

Real-time PCR

Total RNA was extracted from the cells using Total RNA Extraction Kit (BioTeke Corporation,

Beijing, China). RNA (1 μg) was reverse transcribed into cDNA. The gene expression of IL-10 was determined by real-time PCR using SYBR Green I (Solarbio, Beijing, China) in BIONEER *Exicycler*™ 96 (Daejeon, Korea) following the amplification program: 10 min at 95°C and 40 cycles of 10 s at 95°C, 20 s at 60°C and 30 s at 72°C. Primers used in this study were: IL-10-Forward, 5'-TGGAGGACTTTAAGGGTTAC-3', Reverse, 5'-GATGTCTGGGTCTTGGTTC-3'; β-actin-Forward, 5'-CTTAGTTGCGTTACACCCTTTCTTG-3', Reverse, 5'-CTGTCACCTTCACCGTTCCAGTTT-3'. Relative gene expression was determined using $2^{-\Delta\Delta Ct}$ method [29].

Cell culture

Mouse fibroblasts NIH-3T3 were purchased from cell bank at Chinese Academic of Sciences (Shanghai, China). The cells were cultured in DMEM (Gibco) supplemented with 10% FBS (GE Healthcare HyClone) and $NaHCO_3$ (3.7 g/L) in a 5% CO_2 incubator at 37°C.

Crystal violet staining

NIH-3T3 cells were harvested by centrifugation at 48 and 96 h and resuspended in 1 ml PBS. Then, cell suspension (10 μl) was diluted in 100 μl PBS, stained with crystal violet at room temperature for 2 min and added onto the Nageotte Counting Chamber. The cell numbers of living cells and total cells were counted under a microscope (Motic, Xiamen, China).

Cell apoptosis

Annexin V-FITC Apoptosis Detection Kit purchased from KeyGEN BioTECH (Nanjing, China) was used to detect cell apoptosis. The cells were harvested, washed with PBS and resuspendend in Binding buffer. Next, the cells were stained with 5 μl Annexin V-FITC and 5 μl Propidium Iodide (PI). After 15 min of incubation in the dark, the samples were analyzed by flow cytometer (BD).

Transwell invasion assay

Cell invasion was examined by Transwell assay at 24 h. NIH-3T3 cell suspension (2×10^4 cells) was seeded into the upper chamber pre-coated with Matrigel (BD) in 24-well plates and 800 μl DMEM plus 20% FBS was added into the lower chamber. After culturing at 37°C for 24 h, the cells were washed with PBS and fixed with 4% paraformaldehyde (Sinopharm, Shenyang, China). The cell nuclei were stained with crystal violet (Amresco, Solon, OH, USA). The invaded cell number was counted (Motic).

Western blot

The cells were homogenized and lysed in RIPA lysis buffer (Beyotime, Haimen, China) containing proteinase inhibitor PMSF (Beyotime). The supernatants (total proteins) were obtained by centrifugation. Then, equal amount of total proteins (40 μg) were loaded and separated by SDS-PAGE. The proteins were transferred onto PVDF membranes (Millipore, Billerica, MA, USA). After blocking with BSA or nonfat milk, the membranes were incubated overnight at 4°C with primary antibodies against MMP-2 (1:400, Boster, Wuhan, China), MMP-9 (1:400, Boster), STAT3 (1:200, Santa Cruz, Dallas, Texas, USA), p-STAT3 (1:200, Santa Cruz), ERK (1:500, Bioss, Beijing, China) and p-ERK (1:500, Bioss), followed by incubation with IgG-HRP (1:5000, Beyotime). The proteins were enhanced by ECL reagent (7Sea, Shanghai, China) and quantified using Gel-Pro-Analyzer 4.0 (Media Cybernetics, Rockville, MD, USA).

Thermal injury mouse model

C57BL/6 mice (weighting 18 to 20 g) enrolled in this study were purchased from Charles River (Beijing, China). Hair was removed from the dorsal surface. The mice were anesthesized by intraperitoneal (i.p.) injection of 10% chloral hydrate (3.5 ml/kg) and the dorsal surface was exposed to hot water more than 80°C for 10 s using a plastic tube with a 2 cm diameter. The mice were divided into five groups randomly (6 mice in each group): (i) PDMSC-norCM group, the mice were injected with 100 μl PDMSC-norCM immediately after thermal injury; (ii) PDMSC-norCM+IL-10 group, the mice received a injection of PDMSC-norCM containing 10 ng/ml IL-10 (PEPROTECH, Rocky Hill, NJ, USA); (iii) PDMSC-hypoCM group, PDMSC-hypoCM was administrated into the mice; (iv) PDMSC-hypoCM+IL-10 antibody group, PDMSC-hypoCM containing IL-10 antibody (PEPROTECH) was inoculated into the mice; (v) control group, the mice were subcutaneously administrated with the same volume of vehicle (DMEM). The mice were sacrificed on day 15. The scar tissues

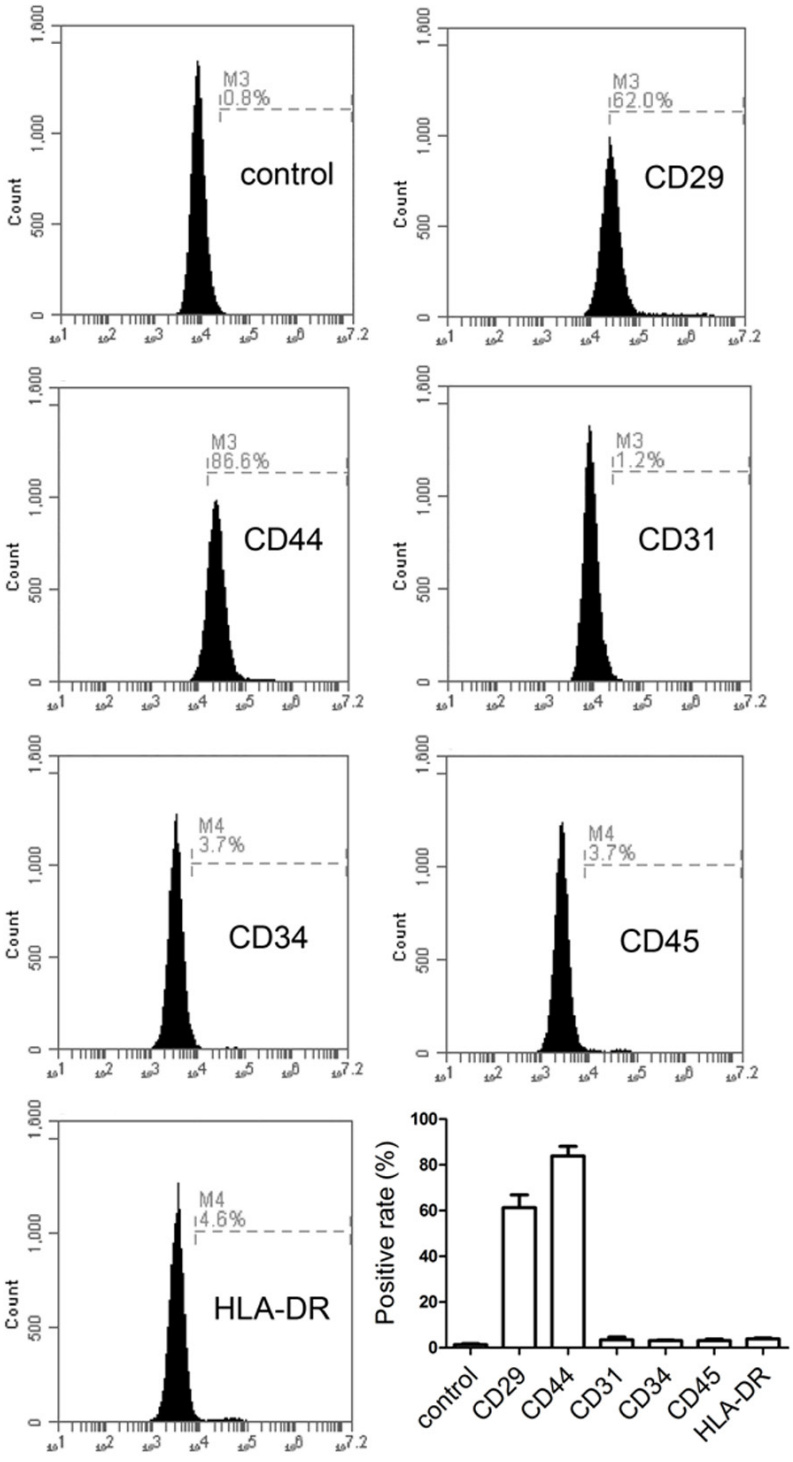

Figure 1. Characterization of placenta-derived mesenchymal stem cells (PDMSCs). Mouse PDMSCs were isolated from the mouse placental tissues and identified by flow cytometer using antibodies against CD29, CD31, CD34, CD44, CD45 and HLA-DR.

were immediately excised and fixed in 4% paraformaldehyde.

Immunohistochemical staining

The paraffin-embedded tissue sections were sliced into 5-μm sections, deparaffinized in xylene solution and rehydrated in graded ethanol (95%, 85% and 75% ethanol for 2 min) (Sinopharm). After heat-induced epitope retrieval, the sections were incubated with H_2O_2 (Sinopharm) for 15 min at room temperature and blocked with goat serum (Solarbio). Subsequently, the sections were treated with anti-α-SMA antibody (1:200, Boster), anti-Ki67 antibody (1:300, Abcam, Cambridge, MA, USA) and anti-F4/80 antibody (1:50, Santa Cruz) at 4°C overnight followed by incubated with biotin-labeled goat anti-rabbit/mouse IgG (1:200; Beyotime) and horseradish peroxidase (HRP)-labeled avidin (1:200, Beyotime). Then, the sections were washed with PBS, developed with DAB solution and counterstained with haematoxylin (Solarbio). Images were photographed under an Olympus DP73 microscope (Tokyo, Japan). The optical density was analyzed using Image-Pro Plus software (Media Cybernetics, Rockville, MD, USA)

Statistical analysis

Results are expressed as Mean ± SD. Statistical analysis was performed by one-way ANOVA followed by Bonferroni post hoc tests using the software Graphpad Prism 4 (Graphpad Prism Software, La Jolla, CA, USA). $P<0.05$ was considered statistically significant.

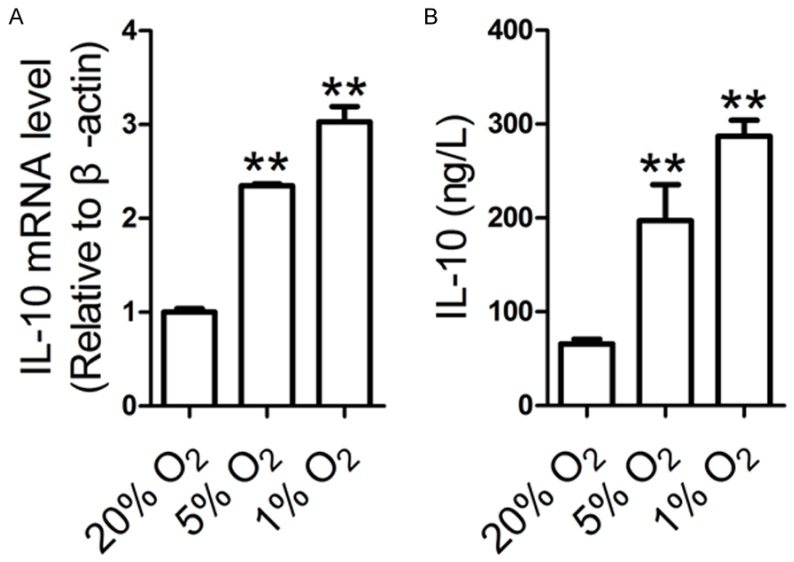

Figure 2. IL-10 expression in hypoxia-treated PDMSCs. PDMSCs was cultured under normoxic and hypoxic conditions. The cells and the supernatant were collected 3 days later. A. The level of IL-10 in PDMSCs was measured by Real-time PCR. B. IL-10 level in the cell culture supernatant was examined by ELISA. $^{**}P<0.01$ vs. 20% O_2 group.

Results

Identification of PDMSCs

PDMSCs at passage 3 were identified by flow cytometry. The results showed that PDMSCs were positive for CD29 and CD44 compared with the control, while negative for CD31, CD34, CD45 and HLA-DR (**Figure 1**).

Expression of IL-10 in hypoxia-treated PDMSCs

IL-10, an anti-fibrotic cytokine, plays an important role in scarless healing [18]. Hypoxia can increase IL-10 expression in ADMSCs [22]. Previous research demonstrated that hypoxia-preconditioned MSCs inhibited cardiac fibroblast activation and pulmonary fibrosis [23, 24]. Therefore, we measured IL-10 expression in PDMSCs and cell culture supernatant after being cultured for 3 days under normoxia and hypoxia. Real-time PCR results showed that IL-10 mRNA levels in the 5% and 1% O_2 groups were 2.35-fold and 3.03-fold higher than that in the 20% O_2 group (**Figure 2A**). ELISA results showed that hypoxia (5% and 1% O_2) increased IL-10 level (ng/L) from 65.79±5.12 to 197.29±38.09 (5% O_2) and 287.05±17.17 (1% O_2) compared with normoxic environments (**Figure 2B**).

PDMSC-hypoCM and IL-10 inhibit proliferation and invasion of NIH-3T3 cells and promote apoptosis in vitro

Crystal violet staining was performed to detect the viable cells. The results showed that the viable cells in the PDMSC-norCM group were markedly decreased after incubation with IL-10 (**Figure 3A**). Additionally, the viable cell number in the PDMSC-hypoCM group was lower than that in the PDMSC-norCM group. However, the effect of PDMSC-hypoCM can be blocked by incubation with the neutralizing antibody against IL-10. We further analyzed the apoptotic rate in each group using Annexin V-FITC/PI staining. As shown in **Figure 3B**, the apoptotic rates of PDMSC-hypoCM group and PDMSC-norCM+IL-10 group were higher than that of the PDMSC-norCM group. Compared with the PDMSC-hypoCM group, IL-10 antibody treatment significantly decreased the apoptotic rate. Transwell invasion assay revealed that the invaded cell number in the PDMSC-norCM+IL-10 group or the PDMSC-hypoCM group was significantly decreased compared with that in the PDMSC-norCM group (**Figure 3C**). IL-10 antibody abrogated the inhibitory effect of PDMSC-hypoCM on cell invasion capability. We further measured the expression of invasion-related proteins by Western blot. The results showed that both IL-10 treatment and PDMSC-hypoCM significantly reduced MMP-2 and MMP-9 expression levels (**Figure 3D**). These protein levels were significantly enhanced when IL-10 was neutralized by IL-10 antibody, indicating that PDMSC-hypoCM inhibits survival and invasion and promotes apoptosis of NIH-3T3 cells via IL-10.

PDMSC-hypoCM and IL-10 inhibit the expression of α-SMA, Ki67 and F4/80 in scar tissues in vivo

We measured α-SMA, Ki67 and F4/80 levels in scar tissues using Immunohistochemical stain-

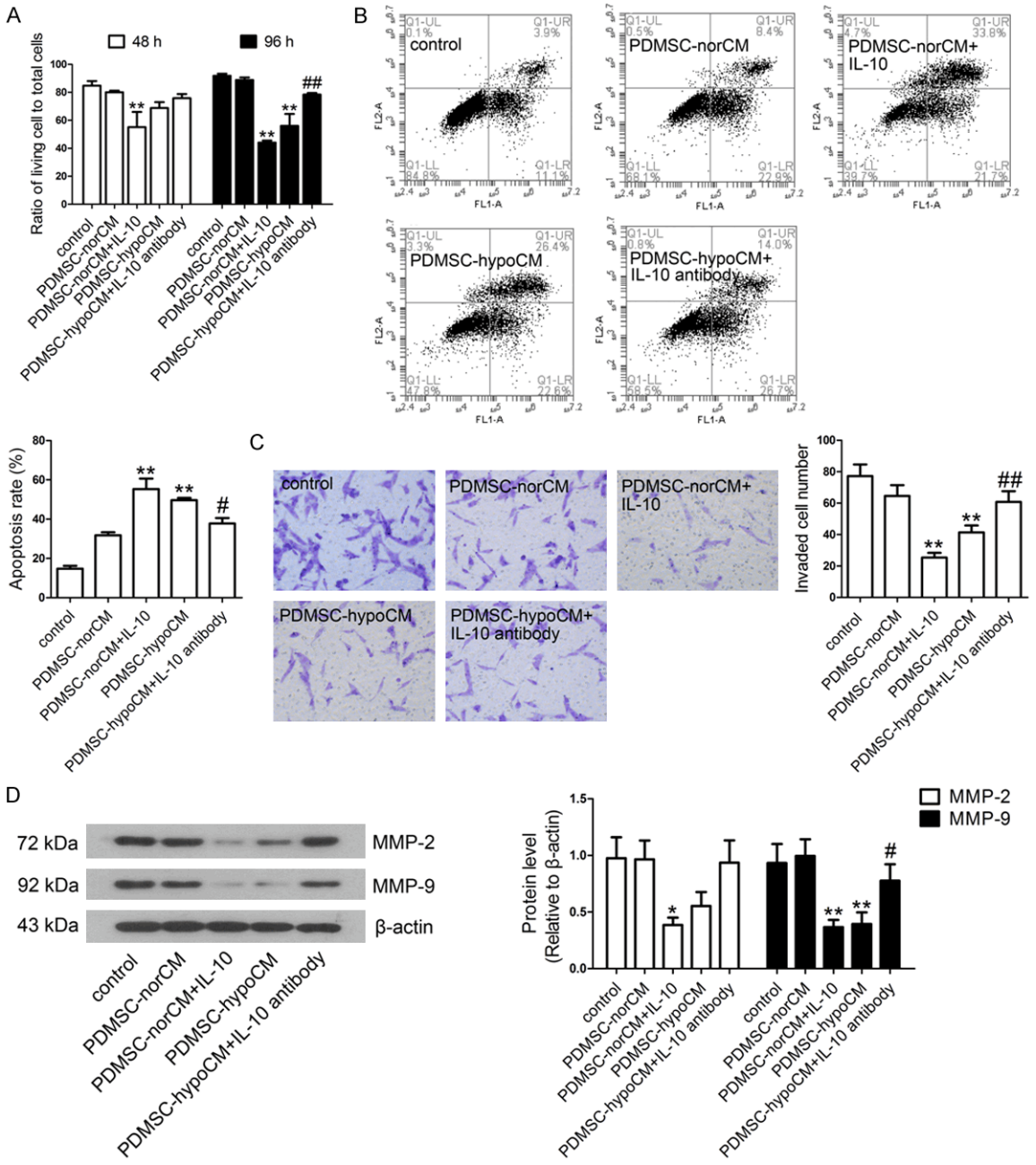

Figure 3. PDMSC-hypoCM inhibited cell survival and invasion of mouse fibroblasts NIH-3T3 and promoted cell apoptosis via IL-10 *in vitro*. A. NIH-3T3 cells were cultured in conditioned medium with/without IL-10 or IL-10 antibody. Cell survival was evaluated by crystal violet staining at 48 and 96 h. B. Cell apoptosis was detected using Annexin V-FITC/PI staining. C. Cell invasion was examined by Transwell invasion assay. The number of invaded cells was counted under a microscope. D. Total proteins were extracted from NIH-3T3 cells after indicated treatment. The expression levels of MMP-2 and MMP-9 were determined by Western blot. **P*<0.05 and ***P*<0.01 vs. PDMSC-norCM group. #*P*<0.05 and ##*P*<0.01 vs. PDMSC-hypoCM group.

ing. The results (**Figure 4**) showed that the expression levels of α-SMA, Ki67 and F4/80 in scar tissues of the PDMSC-norCM+IL-10 group and PDMSC-hypoCM group were significantly lower than those of the PDMSC-norCM group. However, treatment with IL-10 specific antibody restored the decreased levels of α-SMA, Ki67 and F4/80 in the PDMSC-hypoCM group. The

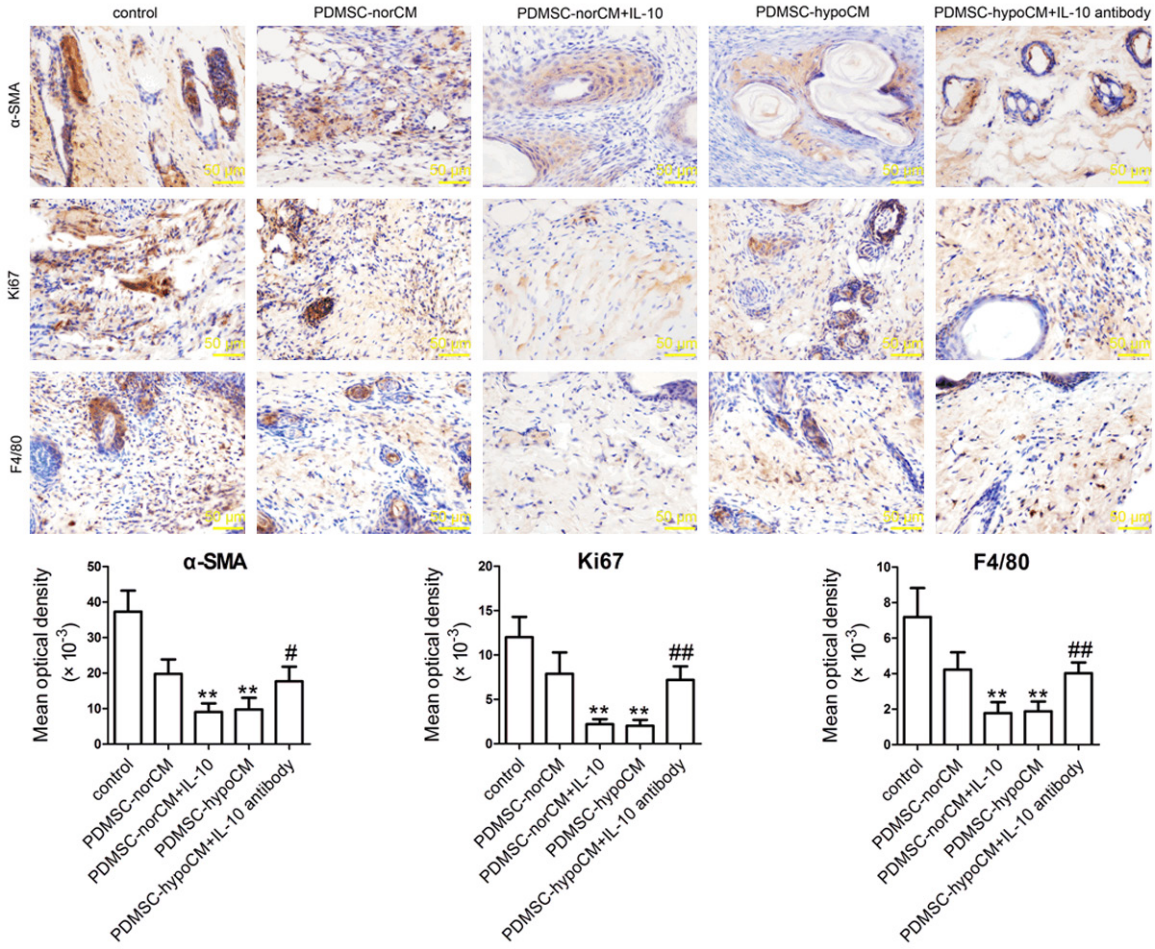

Figure 4. PDMSC-hypoCM inhibited the α-SMA, Ki67 and F4/80 levels in scar tissues via IL-10 *in vivo*. The scar tissues were excised from the mice on day 15 and total proteins were extracted from the tissues. The levels of α-SMA, Ki67 and F4/80 were evaluated by Immunohistochemical staining. *Scale bars* 50 μm. ***P*<0.01 vs. PDMSC-norCM group. #*P*<0.05 and ##*P*<0.01 vs. PDMSC-hypoCM group.

results indicate that IL-10 is involved in the PDMSC-hypoCM-mediated downregulation of α-SMA, Ki67 and F4/80 in scar tissues.

PDMSC-hypoCM and IL-10 inhibit the phosphorylation of STAT3 and ERK in scar tissues

To evaluate the possible roles of STAT3/ERK signaling and IL-10 in scar formation *in vivo*, we excised scar tissues and determined the expression of STAT3, p-STAT3, ERK and p-ERK using Western blot after animal experiments. The ratios of p-STAT3/STAT3 and p-ERK/ERK in the PDMSC-norCM+IL-10 group were lower than that in the PDMSC-norCM group (**Figure 5**). PDMSC-hypoCM markedly decreased the phosphorylation levels of STAT3 and ERK. IL-10 neutralizing antibody alleviated the inhibition of STAT3 and ERK pathways. The results suggest that IL-10 is involved in the suppression of STAT3 and ERK pathways by PDMSC-hypoCM.

Discussion

Abnormal proliferation of fibroblasts contributes to hypertrophic scar formation and excessive ECM deposition [30]. Currently, mouse NIH-3T3 fibroblasts are widely used to investigate the wound healing activities of drugs *in vitro* [31, 32]. In the present study, we isolated and identified mouse PDMSCs. Then, we investigated the effect of IL-10 addition or PDMSC-hypoCM on the biological characteristics of mouse fibroblasts NIH-3T3 *in vitro* and scar fibroblasts in a mouse model of thermal injury *in vivo* using IL-10 neutralizing antibody. We then evaluated the activation of STAT3 and ERK pathways in scar tissues.

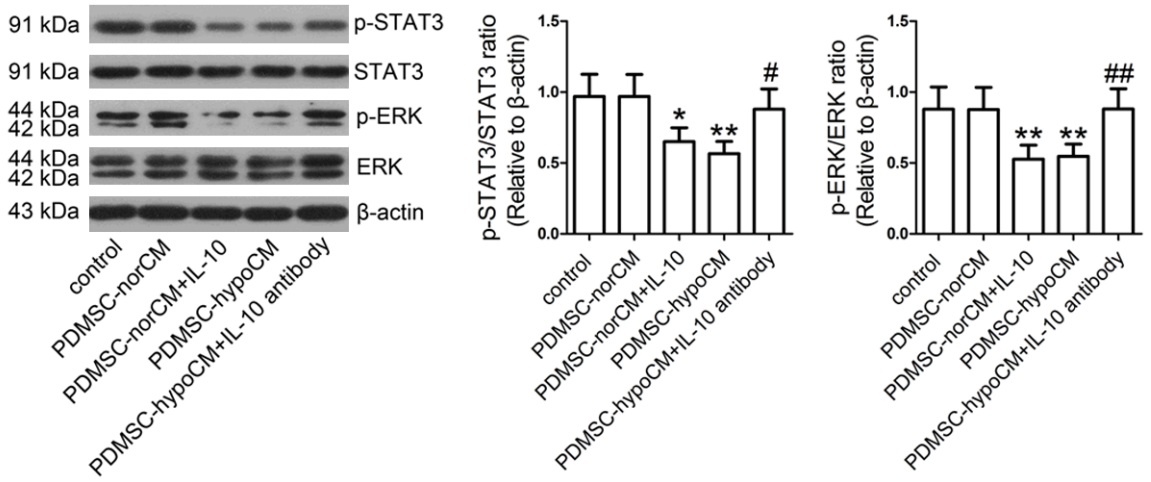

Figure 5. STAT3 and ERK pathways were inhibited by PDMSC-hypoCM *in vivo*. The protein levels of p-STAT3, STAT3, p-ERK and ERK were measured by Western blot. **P*<0.05 and ***P*<0.01 vs. PDMSC-norCM group. #*P*<0.05 and ##*P*<0.01 vs. PDMSC-hypoCM group.

Interleukin (IL)-10, which was identified by Mosmann et al., is an anti-inflammatory cytokine [33]. Recently, several researchers reported that IL-10 played a vital role in reducing hypertrophic scar [20, 34]. Therefore, we measured IL-10 expression in PDMSCs under normoxic and hypoxic conditions. We found that hypoxia increased the mRNA level and the secretion of IL-10 from mouse PDMSCs, which was consistent with previous reports [35].

Fibroblasts play an important role in scar formation. Fibroblasts can migrate to the wound, transdifferentiate into myofibroblasts and synthesize ECM during wound healing, which may lead to the formation of hypertrophic scar [36, 37]. Hypoxia has been commonly used as a method for studying the immunomodulatory capabilities of MSCs. Lan et al. demonstrated that hypoxia-preconditioned MSCs alleviated pulmonary fibrosis induced by bleomycin in C57BL/6JNarl mice [24]. Jiang et al. reported that 2% hypoxia enhanced IL-10 release in the co-culture supernatant of human gingiva-derived MSCs and PBMCs (peripheral blood mononuclear cells) and thereby suppressed the proliferation of PBMCs [38]. MMP-2 and MMP-9 play an important role in cell invasion and migration [39]. However, the effect of PDMSC-hypoCM on the biological properties of fibroblasts remains unknown. In our study, we found that PDMSC-hypoCM and IL-10 treatment inhibited cell survival and invasion of mouse fibroblasts NIH-3T3 and promoted cell apoptosis, accompanied by the decreased levels of MMP-2 and MMP-9. The results pointed out that these effects might be due to the addition of IL-10 in PDMSC-norCM or the release of IL-10 from hypoxia conditioned PDMSCs. Therefore, we using IL-10 neutralizing antibody to test our hypothesis. As expected, incubation with neutralizing antibody against IL-10 reversed the effect of PDMSC-hypoCM. The above results indicate that IL-10 is involved in cell survival, apoptosis and invasion of fibroblasts.

α-SMA is a myofibroblast marker and contributes to the generation of contractile force in myofibroblasts [40]. Myofibroblasts have been demonstrated to participate in hypertrophic scar formation [41]. A previous research showed that adipose-derived stem cells (ADSCs) treatment reduced hypertrophic scar in rabbit ear, with the suppression of α-SMA and collagen [42]. Ren et al. found that induced pluripotent stem cells-conditioned medium (iPSC-CM) significantly reduced α-SMA expression and thus inhibited the activation of hypertrophic scar fibroblasts [43]. Ki67 is a commonly used marker of cell proliferation [44]. Our results showed that PDMSC-hypoCM and IL-10 significantly decreased the expression of α-SMA, Ki67 and F4/80 (known as the macrophage marker), whereas the effect of PDMSC-hypoCM was reversed by IL-10 neutralizing antibody. The results suggest that PDMSC-hypoCM may suppress the proliferation and transdifferentia-

tion of fibroblasts and inhibit the infiltration of macrophages via IL-10.

STAT3 signaling pathway is associated with cell survival, proliferation and invasion [45]. In addition, the activation of STAT3 also elevates the expression of pro-fibrotic genes and thus regulates the cell function of fibroblasts in fibrotic lung diseases [46]. Previous studies demonstrated that inhibition of STAT3 decreased the collagen production of cardiac fibroblasts in a rat model of cardiac hypertrophy and reduced the disposition of ECM in renal interstitial fibrosis in mice [47, 48]. Additionally, ERK signaling pathway is critical for fibrosis and collagen deposition [49, 50]. Therefore, we hypothesized that STAT3 and ERK signaling pathways were associated with hypertrophic scar formation. Our results showed that PDMSC-hypoCM and IL-10 in PDMSC-norCM significantly decreased p-STAT3/STAT3 and p-ERK/ERK ratios, whereas the effect of PDMSC-hypoCM was reversed by IL-10 neutralizing antibody. The results indicate that PDMSC-hypoCM may suppress the STAT3 and ERK signaling pathways to reduce scar formation via IL-10.

In conclusion, our study demonstrated that PDMSC-hypoCM inhibited scar formation through IL-10, STAT3 and ERK pathways. Our present study provides evidences for the treatment of hypertrophic scar.

Acknowledgements

This study was supported by a grant from the Doctoral Scientific Research Foundation of Liaoning Province (No: 201501003).

Disclosure of conflict of interest

None.

Address correspondence to: Dr. Lili Du, Department of Pathophysiology, College of Basic Medical Science, China Medical University, 77 Puhe Road, Shenyang 110122, People's Republic of China. E-mail: dllbinglishengli@126.com

References

[1] Schwacha MG and Chaudry IH. The cellular basis of post-burn immunosuppression: macrophages and mediators. Int J Mol Med 2002; 10: 239-243.

[2] Yang Q, Orman MA, Berthiaume F, Ierapetritou MG and Androulakis IP. Dynamics of short-term gene expression profiling in liver following thermal injury. J Surg Res 2012; 176: 549-558.

[3] Foubert P, Barillas S, Gonzalez AD, Alfonso Z, Zhao S, Hakim I, Meschter C, Tenenhaus M and Fraser JK. Uncultured adipose-derived regenerative cells (ADRCs) seeded in collagen scaffold improves dermal regeneration, enhancing early vascularization and structural organization following thermal burns. Burns 2015; 41: 1504-1516.

[4] Ding J, Ma Z, Liu H, Kwan P, Iwashina T, Shankowsky HA, Wong D and Tredget EE. The therapeutic potential of a C-X-C chemokine receptor type 4 (CXCR-4) antagonist on hypertrophic scarring in vivo. Wound Repair Regen 2014; 22: 622-630.

[5] Wang X, Chu J, Wen CJ, Fu SB, Qian YL, Wo Y, Wang C and Wang DR. Functional characterization of TRAP1-like protein involved in modulating fibrotic processes mediated by TGF-beta/Smad signaling in hypertrophic scar fibroblasts. Exp Cell Res 2015; 332: 202-211.

[6] Zhu HY, Li C, Zheng Z, Zhou Q, Guan H, Su LL, Han JT, Zhu XX, Wang SY, Li J and Hu DH. Peroxisome proliferator-activated receptor-gamma (PPAR-gamma) agonist inhibits collagen synthesis in human hypertrophic scar fibroblasts by targeting Smad3 via miR-145. Biochem Biophys Res Commun 2015; 459: 49-53.

[7] Kuang R, Wang Z, Xu Q, Liu S and Zhang W. Influence of mechanical stimulation on human dermal fibroblasts derived from different body sites. Int J Clin Exp Med 2015; 8: 7641-7647.

[8] Liu YL, Liu WH, Sun J, Hou TJ, Liu YM, Liu HR, Luo YH, Zhao NN, Tang Y and Deng FM. Mesenchymal stem cell-mediated suppression of hypertrophic scarring is p53 dependent in a rabbit ear model. Stem Cell Res Ther 2014; 5: 136.

[9] Jackson WM, Nesti LJ and Tuan RS. Mesenchymal stem cell therapy for attenuation of scar formation during wound healing. Stem Cell Res Ther 2012; 3: 20.

[10] Tobita M, Tajima S and Mizuno H. Adipose tissue-derived mesenchymal stem cells and platelet-rich plasma: stem cell transplantation methods that enhance stemness. Stem Cell Res Ther 2015; 6: 215.

[11] Garimella MG, Kour S, Piprode V, Mittal M, Kumar A, Rani L, Pote ST, Mishra GC, Chattopadhyay N and Wani MR. Adipose-Derived Mesenchymal Stem Cells Prevent Systemic Bone Loss in Collagen-Induced Arthritis. J Immunol 2015; 195: 5136-48.

[12] Uccelli A, Moretta L and Pistoia V. Immunoregulatory function of mesenchymal stem cells. Eur J Immunol 2006; 36: 2566-2573.

[13] Miao Z, Jin J, Chen L, Zhu J, Huang W, Zhao J, Qian H and Zhang X. Isolation of mesenchymal stem cells from human placenta: comparison with human bone marrow mesenchymal stem cells. Cell Biol Int 2006; 30: 681-687.
[14] Yun HM, Kim HS, Park KR, Shin JM, Kang AR, il Lee K, Song S, Kim YB, Han SB, Chung HM and Hong JT. Placenta-derived mesenchymal stem cells improve memory dysfunction in an Abeta1-42-infused mouse model of Alzheimer's disease. Cell Death Dis 2013; 4: e958.
[15] Chambers DC, Enever D, Ilic N, Sparks L, Whitelaw K, Ayres J, Yerkovich ST, Khalil D, Atkinson KM and Hopkins PM. A phase 1b study of placenta-derived mesenchymal stromal cells in patients with idiopathic pulmonary fibrosis. Respirology 2014; 19: 1013-1018.
[16] Kong P, Xie X, Li F, Liu Y and Lu Y. Placenta mesenchymal stem cell accelerates wound healing by enhancing angiogenesis in diabetic Goto-Kakizaki (GK) rats. Biochem Biophys Res Commun 2013; 438: 410-419.
[17] Shi J, Wan Y, Shi S, Zi J, Guan H, Zhang Y, Zheng Z, Jia Y, Bai X, Cai W, Su L, Zhu X and Hu D. Expression, purification, and characterization of scar tissue neovasculature endothelial cell-targeted rhIL10 in Escherichia coli. Appl Biochem Biotechnol 2015; 175: 625-634.
[18] Shi J, Li J, Guan H, Cai W, Bai X, Fang X, Hu X, Wang Y, Wang H, Zheng Z, Su L, Hu D and Zhu X. Anti-fibrotic actions of interleukin-10 against hypertrophic scarring by activation of PI3K/AKT and STAT3 signaling pathways in scar-forming fibroblasts. PLoS One 2014; 9: e98228.
[19] Dennis KL, Blatner NR, Gounari F and Khazaie K. Current status of interleukin-10 and regulatory T-cells in cancer. Curr Opin Oncol 2013; 25: 637-645.
[20] Kieran I, Knock A, Bush J, So K, Metcalfe A, Hobson R, Mason T, O'Kane S and Ferguson M. Interleukin-10 reduces scar formation in both animal and human cutaneous wounds: results of two preclinical and phase II randomized control studies. Wound Repair Regen 2013; 21: 428-436.
[21] van den Broek LJ, van der Veer WM, de Jong EH, Gibbs S and Niessen FB. Suppressed inflammatory gene expression during human hypertrophic scar compared to normotrophic scar formation. Exp Dermatol 2015; 24: 623-629.
[22] Xu L, Wang X, Wang J, Liu D, Wang Y, Huang Z and Tan H. Hypoxia-induced secretion of IL-10 from adipose-derived mesenchymal stem cell promotes growth and cancer stem cell properties of Burkitt lymphoma. Tumour Biol 2016; 37: 7835-42.
[23] Chen P, Wu R, Zhu W, Jiang Z, Xu Y, Chen H, Zhang Z, Zhang L, Yu H, Wang J and Hu X. Hypoxia preconditioned mesenchymal stem cells prevent cardiac fibroblast activation and collagen production via leptin. PLoS One 2014; 9: e103587.
[24] Lan YW, Choo KB, Chen CM, Hung TH, Chen YB, Hsieh CH, Kuo HP and Chong KY. Hypoxia-preconditioned mesenchymal stem cells attenuate bleomycin-induced pulmonary fibrosis. Stem Cell Res Ther 2015; 6: 97.
[25] Yu J, Yuan X, Liu Y, Zhang K, Wang J, Zhang H and Liu F. Delayed Administration of WP1066, an STAT3 Inhibitor, Ameliorates Radiation-Induced Lung Injury in Mice. Lung 2016; 194: 67-74.
[26] O'Reilly S, Ciechomska M, Cant R and van Laar JM. Interleukin-6 (IL-6) trans signaling drives a STAT3-dependent pathway that leads to hyperactive transforming growth factor-beta (TGF-beta) signaling promoting SMAD3 activation and fibrosis via Gremlin protein. J Biol Chem 2014; 289: 9952-9960.
[27] Nutter FH, Haylor JL and Khwaja A. Inhibiting ERK Activation with CI-1040 Leads to Compensatory Upregulation of Alternate MAPKs and Plasminogen Activator Inhibitor-1 following Subtotal Nephrectomy with No Impact on Kidney Fibrosis. PLoS One 2015; 10: e0137321.
[28] Wang H, Chen Z, Li XJ, Ma L and Tang YL. Anti-inflammatory cytokine TSG-6 inhibits hypertrophic scar formation in a rabbit ear model. Eur J Pharmacol 2015; 751: 42-49.
[29] Livak KJ and Schmittgen TD. Analysis of relative gene expression data using real-time quantitative PCR and the 2(-Delta Delta C(T)) Method. Methods 2001; 25: 402-408.
[30] Yang H, Hu C, Li F, Liang L and Liu L. Effect of lipopolysaccharide on the biological characteristics of human skin fibroblasts and hypertrophic scar tissue formation. IUBMB Life 2013; 65: 526-532.
[31] Kil YS, Park J, Han AR, Woo HA and Seo EK. A new 9,10-dihydrophenanthrene and cell proliferative 3,4-delta-dehydrotocopherols from Stemona tuberosa. Molecules 2015; 20: 5965-5974.
[32] Su Z, Ma H, Wu Z, Zeng H, Li Z, Wang Y, Liu G, Xu B, Lin Y, Zhang P and Wei X. Enhancement of skin wound healing with decellularized scaffolds loaded with hyaluronic acid and epidermal growth factor. Mater Sci Eng C Mater Biol Appl 2014; 44: 440-448.
[33] Ouyang W, Rutz S, Crellin NK, Valdez PA and Hymowitz SG. Regulation and functions of the IL-10 family of cytokines in inflammation and disease. Annu Rev Immunol 2011; 29: 71-109.

[34] Occleston NL, O'Kane S, Goldspink N and Ferguson MW. New therapeutics for the prevention and reduction of scarring. Drug Discov Today 2008; 13: 973-981.
[35] Li Z, Wei H, Deng L, Cong X and Chen X. Expression and secretion of interleukin-1beta, tumour necrosis factor-alpha and interleukin-10 by hypoxia- and serum-deprivation-stimulated mesenchymal stem cells. FEBS J 2010; 277: 3688-3698.
[36] Fan C, Dong Y, Xie Y, Su Y, Zhang X, Leavesley D and Upton Z. Shikonin reduces TGF-beta1-induced collagen production and contraction in hypertrophic scar-derived human skin fibroblasts. Int J Mol Med 2015; 36: 985-991.
[37] He T, Bai X, Yang L, Fan L, Li Y, Su L, Gao J, Han S and Hu D. Loureirin B Inhibits Hypertrophic Scar Formation via Inhibition of the TGF-beta1-ERK/JNK Pathway. Cell Physiol Biochem 2015; 37: 666-676.
[38] Jiang CM, Liu J, Zhao JY, Xiao L, An S, Gou YC, Quan HX, Cheng Q, Zhang YL, He W, Wang YT, Yu WJ, Huang YF, Yi YT, Chen Y and Wang J. Effects of hypoxia on the immunomodulatory properties of human gingiva-derived mesenchymal stem cells. J Dent Res 2015; 94: 69-77.
[39] Tong B, Wan B, Wei Z, Wang T, Zhao P, Dou Y, Lv Z, Xia Y and Dai Y. Role of cathepsin B in regulating migration and invasion of fibroblast-like synoviocytes into inflamed tissue from patients with rheumatoid arthritis. Clin Exp Immunol 2014; 177: 586-597.
[40] Gras C, Ratuszny D, Hadamitzky C, Zhang H, Blasczyk R and Figueiredo C. miR-145 Contributes to Hypertrophic Scarring of the Skin by Inducing Myofibroblast Activity. Mol Med 2015; 21: 296-304.
[41] Wang J, Dodd C, Shankowsky HA, Scott PG and Tredget EE. Deep dermal fibroblasts contribute to hypertrophic scarring. Lab Invest 2008; 88: 1278-1290.
[42] Zhang Q, Liu LN, Yong Q, Deng JC and Cao WG. Intralesional injection of adipose-derived stem cells reduces hypertrophic scarring in a rabbit ear model. Stem Cell Res Ther 2015; 6: 145.
[43] Ren Y, Deng CL, Wan WD, Zheng JH, Mao GY and Yang SL. Suppressive effects of induced pluripotent stem cell-conditioned medium on in vitro hypertrophic scarring fibroblast activation. Mol Med Rep 2015; 11: 2471-2476.
[44] Shui R, Yu B, Bi R, Yang F and Yang W. An interobserver reproducibility analysis of Ki67 visual assessment in breast cancer. PLoS One 2015; 10: e0125131.
[45] Guo C, Su J, Li Z, Xiao R, Wen J, Li Y, Zhang M, Zhang X, Yu D, Huang W, Chen WD and Wang YD. The G-protein-coupled bile acid receptor Gpbar1 (TGR5) suppresses gastric cancer cell proliferation and migration through antagonizing STAT3 signaling pathway. Oncotarget 2015; 6: 34402-34413.
[46] Pechkovsky DV, Prele CM, Wong J, Hogaboam CM, McAnulty RJ, Laurent GJ, Zhang SS, Selman M, Mutsaers SE and Knight DA. STAT3-mediated signaling dysregulates lung fibroblast-myofibroblast activation and differentiation in UIP/IPF. Am J Pathol 2012; 180: 1398-1412.
[47] Mir SA, Chatterjee A, Mitra A, Pathak K, Mahata SK and Sarkar S. Inhibition of signal transducer and activator of transcription 3 (STAT3) attenuates interleukin-6 (IL-6)-induced collagen synthesis and resultant hypertrophy in rat heart. J Biol Chem 2012; 287: 2666-2677.
[48] Pang M, Ma L, Gong R, Tolbert E, Mao H, Ponnusamy M, Chin YE, Yan H, Dworkin LD and Zhuang S. A novel STAT3 inhibitor, S3I-201, attenuates renal interstitial fibroblast activation and interstitial fibrosis in obstructive nephropathy. Kidney Int 2010; 78: 257-268.
[49] Sonin DL, Wakatsuki T, Routhu KV, Harmann LM, Petersen M, Meyer J and Strande JL. Protease-activated receptor 1 inhibition by SCH79797 attenuates left ventricular remodeling and profibrotic activities of cardiac fibroblasts. J Cardiovasc Pharmacol Ther 2013; 18: 460-475.
[50] Lim IJ, Phan TT, Tan EK, Nguyen TT, Tran E, Longaker MT, Song C, Lee ST and Huynh HT. Synchronous activation of ERK and phosphatidylinositol 3-kinase pathways is required for collagen and extracellular matrix production in keloids. J Biol Chem 2003; 278: 40851-40858.